



Original Research

Ascorbic acid analogue 6-Deoxy-6-[¹⁸F] fluoro-L-ascorbic acid as a tracer for identifying human colorectal cancer with SVCT2 overexpression



Peng He^{a,1}, Bing Zhang^{a,1}, Yuan Zou^{b,1}, Yan Zhang^c, Zhihao Zha^d, Yali Long^a, Jia Qiu^a, Wanqing Shen^a, Xiaoping Lin^{e,*}, Zhoulei Li^{a,*}, Xiangsong Zhang^{a,*}

^a Department of Nuclear Medicine & Guangdong Engineering Research Center for Translational Application of Medical Radiopharmaceuticals, The First Affiliated Hospital of Sun Yat-Sen University, Guangzhou 510080, China

^b Department of Ultrasound Medicine & Ultrasonic Medical Engineering Key Laboratory of Nanchong City, Affiliated Hospital of North Sichuan Medical College, Nanchong 637000, China

^c Department of Physiology and Pathophysiology, Capital Medical University, Beijing 100069, China

^d Department of Radiology, University of Pennsylvania School of Medicine, Philadelphia, Pennsylvania

^e Department of Nuclear Medicine, State Key Laboratory of Oncology in South China, Collaborative Innovation Center for Cancer Medicine, Sun Yat-sen University Cancer Center, Guangzhou 510060, China,

ARTICLE INFO

Keywords:

L-ascorbic acid

SVCT2

Positron emission tomography

¹⁸F-DFA

Colorectal cancer

ABSTRACT

L-ascorbic acid (AA) was reported to have an anti-cancer effect over 40 years. In recent years, several ongoing clinical trials are exploring the safety and efficacy of intravenous high-dose AA for cancer treatment. The lack of appropriate imaging modality limits the identification of potentially suitable patients for AA treatment. This study focuses on identifying AA-sensitive tumor cells using molecular imaging. 6-Deoxy-6-[¹⁸F] fluoro-L-ascorbic Acid (¹⁸F-DFA), a structural analog of AA, was synthesized and labeled to visualize the metabolism of AA *in vivo*. Colorectal cancer (CRC) cell lines with high and low expression of sodium-dependent vitamin C transporters 2 (SVCT2) were used for a series of cellular uptake tests. PET imaging was performed on xenograft tumor-bearing mice. More AA uptake was observed in CRC cells with high SVCT2 expression than in cells with low SVCT2 expression. The substrate (unlabeled AA) can competitively inhibit the ¹⁸F-DFA tracer uptake by CRC cells. The biodistribution of ¹⁸F-DFA in mice showed high radioactivity was seen in organs such as adrenal glands, kidneys, and liver that were known to have high concentrations of AA. Both PET imaging and tissue distribution showed that cancer cells with high SVCT2 expression enhanced the accumulation of ¹⁸F-DFA in mice after tumor formation. Immunohistochemistry was used to verify the corresponding results. As a radiotracer, ¹⁸F-DFA can provide powerful imaging information to identify tumor with high affinity of AA, and SVCT2 can be a potential biomarker in this process.

Introduction

L-ascorbic acid (vitamin C, AA) is a water-soluble vitamin and one of the most important antioxidants [1]. Several preclinical studies have shown that pharmacological AA can kill cancer cells *in vitro* and inhibit tumor growth *in vivo* [2, 3]. Recent studies have focused on the beneficial effect of intravenous high-dose AA administration in cancer treatment [4]. The mechanism by which AA selectively kills malignant tumor cells while sparing normal cells remains unclear. It depends on a variety of factors, including different types of tumors, tumor heterogeneity, and tumor dependency on specific pathways, considering a wide range of processes affected by AA [2].

Two families of transporters [5], namely, solute carrier family 23 (SLC23), which is mainly composed of sodium-dependent vitamin C transporters (SVCTs) 1 and 2, and solute carrier family 2 (SLC2) of glucose transporters (GLUTs), mediate the transport of AA into cells. GLUTs transport the oxidized form of vitamin C (dehydroascorbic acid, DHA), which exists at a negligible physiological level [6]. SVCT1 and SVCT2 can transport ascorbate from extracellular micromolar concentrations to intracellular millimolar concentrations against a concentration gradient [7]. SVCT2 is widely distributed in the body and is known to be the major vitamin C transporter [8]. Mice with SVCT2 deficiency lack AA and die at birth [9]. Studies have also shown that the expression of SVCT2 is directly related to the anticancer activity of AA in cancer

* Corresponding authors.

E-mail addresses: linxp@susucc.org.cn (X. Lin), lizhlei3@mail.sysu.edu.cn (Z. Li), zhxiangs@mail.sysu.edu.cn (X. Zhang).

¹ These authors contributed equally to this work.

cells [10,11]. Cancer cells with high SVCT2 expression are more sensitive to AA treatment than those with low SVCT2 expression. SVCT2 was considered to be a potential biomarker for AA and cetuximab treatment in patients with colorectal cancer (CRC) [12]. Some studies have also shown that increased expression of mitochondrial SVCT2 intracellular form is a common feature of all human cancers [13]. Therefore, a study of the mechanisms of extracellular and intracellular transport and accumulation of AA can provide valuable insights on the therapeutic anti-cancer effects of AA.

Molecular imaging is a non-invasive method for effectively monitoring biomolecules at the cellular or subcellular level [14]. Positron emission tomography (PET) is ideal among the molecular imaging methods currently available. PET can provide a new viewpoint for studying the pathophysiology of the tumor-bearing organisms [15]. AA radiolabeled compounds using PET imaging can reveal AA accumulation in organ tissues [16]. In recent years, several studies have focused on AA structural analogs labeled with radionuclides emitting positrons such as ^{18}F , ^{125}I , ^{131}I , and ^{11}C , ^{14}C for this purpose [15,17–20]. The atomic coordinates, bond lengths and angles, hydrogen coordinates, anisotropic and isotropic displacement parameters of 6-Deoxy-6-fluoro-L-ascorbic acid are similar to native AA [21]. Moreover, 6-Deoxy-6-fluoro-L-ascorbic acid has the same transport and accumulation mechanism as AA, but not DHA [22]. Therefore, 6-deoxy-6-fluoro-L-ascorbic acid can be an ideal compound to study the cumulative process of intracellular AA. One-pot synthesis of 6-deoxy-6- ^{18}F fluoro-L-ascorbic acid (^{18}F -DFA) is formed by nucleophilic displacement of a cyclic sulfate with no-carrier-added [^{18}F] fluoride ion [15].

Currently, several ongoing clinical trials are investigating the safety and efficacy of high-dose intravenous AA for the treatment of various types of cancers [2]. With the revived clinical interest in AA as a cancer therapy, we use ^{18}F -DFA as a positron labeling analog of AA, aiming to provide useful information to identify tumors suitable for high-dose AA therapy. The results of *in vitro* and *in vivo* analyses of this novel metabolic tracer are reported in this study.

Materials and methods

Tracer production

All reagents used for chemical synthesis were commercial products and were used without further purification unless otherwise indicated. The synthesis of precursor cyclic sulfate (2), reference standard compound (3), and [^{18}F] DFA ([^{18}F] 3) is outlined in Scheme 1, as described in previous reports [15]. The supplementary information contains detailed procedures [23–25]. Chemical identification of the purified product co-injection with DFA was carried out by high-performance liquid chromatography (HPLC), (3), using a UV/Vis detector at 254 nm and a γ -ray radio detector (Fig. S1). HPLC condition was used: Ascentis C18 column (150 \times 4.6 mm, 5 μm), Mobile phase: 50 mM phosphate-buffered saline (PBS), pH = 6, 1 mL/min. Retention time: [^{18}F] DFA = 3.0–3.5 min, [^{18}F] fluoride = 1.5–2.0 min. The radiochemical yield was 20–33% ($n = 10$) with a radiochemical purity of > 99%.

Cell culture and reagents

The human CRC cell lines SW480, SW620, LoVo, HCT116, and HCT8 were confirmed to be significantly different in SVCT2 expression in previous literature [12,26]. Cells provided by The Kunming Cell Bank, Chinese Academy of Sciences. To authenticate all the cell lines, short tandem repeats (STRs) profiling was used. They were cultured in RPMI 1640 medium (HCT116 and HCT8 cells), DMEM medium (SW480 cells), Ham's F-12 K medium (LoVo cells), and Leibovitz's L-15 medium (SW620 cells) supplemented with 10% fetal bovine serum (FBS) and 1% penicillin/streptomycin (MRC, China) according to the instructions of the provider. All cell lines were cultured at 5% CO_2 in a humidified incubator at 37 $^\circ\text{C}$ and were routinely passaged at confluence. All

reagents used in this study were sourced from Thermo Fisher Scientific unless otherwise stated. All cell-based experiments were repeated twice.

In vitro cellular uptake and substrate-competitive inhibition studies

The cellular uptake of ^{18}F -DFA was studied using various CRC cell lines described earlier. Tumor cells were plated in 6-well plates at an initial density of 3.0×10^5 cells per well. The medium was replaced with PBS with the same pH containing Na^+ after 24 h to 48 h; and 0.037MBq ($1\mu\text{Ci}$) ^{18}F -DFA was added to the individual wells and incubated at 37 $^\circ\text{C}$ for 30 min. The medium was sucked out at the end of the incubation and cells were washed twice using 1 mL of ice-cold PBS to clean up free tracer. The aspirated medium and PBS were collected into a tube and labeled as the extracellular fluid tube (Tube A). Cells were detached from the well using 0.2 mL 0.25% trypsin (MRC), washed twice with 1 mL of ice-cold PBS, and cell-containing fluid was collected into another tube labeled as the cellular fluid tube (Tube B). The radioactivity of each tube was measured using a 2480 WIZARD² γ -counter (PerkinElmer, USA). The ratio of Tube B activity counts to the total counts of Tube A and Tube B was the cellular tracer uptake ratio. BCA protein assay (CWBIO, China) using cells in Tube B was used to determine the protein concentration. Finally, the percentage of cellular uptake was standardized to 100 μg of protein. To characterize the transport of ^{18}F -DFA, substrate-competitive inhibition studies using unlabeled L-AA and structural analogs (dehydroascorbic acid, DHA) were conducted in the five CRC cell lines listed above. The specific operation steps and the calculation method of uptake rate were performed as described earlier.

Animal models

The Committee on the Ethics of Animal Experiments of the First Affiliated Hospital, Sun Yat-sen University approved the use of animals in this study (approval NO. 2019–431). All the experimental mice were placed in a sterile environment with a normal light/dark circadian rhythm; and access to food and water *ad libitum*. The 4–6 weeks female BALB/c nude mice ($n = 40$) were prepared in the Nanjing biomedical research institute of Nanjing University (License NO. SCXK2018–0008). Approximately 7×10^6 HCT8 or SW620 cells were inoculated into the bilateral anterior armpits of nude mice; and the mice were monitored daily. It took 14–21 days for the tumors to reach a suitable size of 10 mm. Before the experiments, all the animals were subjected to fasting for 8 h. At the end of the image data collection, bilateral tumors were collected for immunohistochemical analysis.

In vivo biodistribution study in normal mice

To test the ^{18}F -DFA as a tumor PET imaging agent, this tracer was first tested in normal male BALB/c nude mice (20–25 gs). For the biodistribution analysis, five mice were used per group. The mice were anesthetized using 1.0% pentobarbital sodium (50 mg/kg, intraperitoneal injection, i.p) and tail intravenous injection with 0.1 mL sterile water containing 2.22MBq ($60\mu\text{Ci}$) of ^{18}F -DFA was performed. Then, these mice with radiopharmaceuticals were sacrificed under anesthesia at 30, 60, 90, and 120 min. The organs of interest were removed, weighed, and a 2480 WIZARD² γ -counter was used to measure radioactivity of organs. The percentage of the injected dose per sample gram (% ID/g) was determined by comparing the tissue activity count to 1.0 percent of the initial dose count. The initial dose consisted of 100-fold diluted injected substance aliquots measured at the same rate.

In vivo biodistribution study in tumor-bearing mice

Bilateral xenograft tumor model was established as described earlier. Ten tumor-bearing mice were used to evaluate the biological distribution of ^{18}F -DFA; and the radiopharmaceuticals injection method was

as mentioned above. The mice were sacrificed under anesthesia at 30 and 60 min, respectively. Bilateral tumors and organs of interest were removed, weighed and the radioactivity measured using a 2480 WIZARD2 γ -counter. The %ID/g was calculated using the method described earlier.

Micro-PET studies and image analysis

A Micro-PET scanner (Siemens, Germany) equipped with the Inveon Research Workplace 4.1 software was used to obtain the images of tumor-bearing mice. Before imaging, all mice were anesthetized and placed on a heating pad to maintain their body temperature throughout the process. To analyze the dynamic PET imaging of tumor-bearing mice ($n = 2$), 3.7 MBq (100 μ Ci) of ^{18}F -DFA was injected. After intravenous tracer injection, data was collected continuously for 2 h (dynamic, 5 min/frame). Static PET imaging studies using 3.7 MBq of ^{18}F -DFA on tumor-bearing mice ($n = 5$) were conducted 60 min after injection. To obtain an imaging region-of-interest (ROI)-derived %ID/g, the images were reconstructed by the previously described method [27].

Ex vivo PET study in mice bearing xenograft tumors

After fixing the tumor-bearing mouse, 3.7 MBq ^{18}F -DFA was injected intravenously. The mouse was sacrificed by cervical dislocation under anesthesia, 60 min after injection. The bilateral tumors and organs of interest were removed and placed on a 5.0×12.0 cm cardboard that matched the size of the scanning bed. The cardboard containing the organs was then placed in the micro PET scanner and imaging commenced. After 10 min of scanning, data was analyzed and reconstructed using the software from the vendor.

Western blot analysis

Western blot analysis was performed using the above-listed CRC cells. Protein concentration was determined using the protein determination dye method based on bovine serum albumin (Merck, Germany) after the cells were collected, washed, pelleted, and lysed. For immunoblotting, 30 μ g protein was separated from each lane on 8% gradient ready-made SDS gel and transferred to polyvinylidene fluoride membrane (Millipore, USA). The anti-SVCT2 antibody (ab229802, Abcam, USA) was diluted to 1:1000 in a closed buffer; and incubated with the membrane overnight at 4 °C. The membrane was then incubated with the secondary antibody. A Pierce Quick Western Blot Kit was used to develop the resulting imprint and then transmitted to film. In order to ensure that the target band of SVCT2, we referred to the official instructions given by the antibody supplier Abcam and refer to the protein database UniProt (www.uniprot.org). Finally, we determined that the SVCT2 protein band should be near 70 kDa.

Statistical analysis

Quantitative data were represented as mean \pm standard deviation, and differences between the two groups were calculated using independent-sample *t*-test (two-tailed) in Prism software (version 8; GraphPad Software). Linear regression analysis (SPSS 22.0) was used to show the relationship between the results of Western blotting and radiotracer uptake of AA. Statistical significance was set at $P < 0.05$ *, < 0.01 ** or < 0.001 *** representing significance between exposure conditions.

Results

Association of SVCT2 expression and ^{18}F -DFA cellular uptake in CRC cells

In vitro cellular uptake experiments were conducted to examine the uptake of ^{18}F -DFA in various human CRC cell lines. To characterize the

Table 1

In tissue biodistribution of 6-Deoxy-6- ^{18}F fluoro-L-ascorbic Acid in BALB/c nude mice after intravenous injection.

Organ	30min	60min	90min	120min
Brain	0.51 \pm 0.25	0.60 \pm 0.19	0.64 \pm 0.05	0.67 \pm 0.08
Blood	0.48 \pm 0.20	0.42 \pm 0.12	0.38 \pm 0.05	0.29 \pm 0.03
Heart	1.27 \pm 0.19	1.36 \pm 0.47	1.39 \pm 0.28	1.28 \pm 0.35
Lung	6.23 \pm 2.29	8.35 \pm 1.34	8.64 \pm 0.46	8.05 \pm 1.13
Liver	8.02 \pm 1.35	6.99 \pm 1.16	5.71 \pm 0.67	5.47 \pm 0.76
Pancreas	2.79 \pm 0.92	2.60 \pm 1.70	2.71 \pm 0.28	2.55 \pm 0.69
Spleen	3.55 \pm 1.19	4.37 \pm 1.31	2.24 \pm 0.67	2.64 \pm 0.94
Adrenals	11.6 \pm 2.06	14.2 \pm 2.43	13.6 \pm 1.91	11.4 \pm 1.55
Kidneys	9.45 \pm 1.93	7.17 \pm 1.82	6.87 \pm 1.37	5.44 \pm 1.16
Intestine	7.69 \pm 1.63	8.33 \pm 0.93	7.75 \pm 0.43	7.63 \pm 1.19
Stomach	2.13 \pm 0.64	2.37 \pm 0.71	2.53 \pm 0.26	2.94 \pm 0.49
Muscle	0.49 \pm 0.18	0.55 \pm 0.19	0.64 \pm 0.16	0.57 \pm 0.16
Bone	1.02 \pm 0.39	1.12 \pm 0.11	1.30 \pm 0.08	1.44 \pm 0.16

Data represented as %ID/g, mean \pm SD (5 mice per time point).

difference of these cell lines, Western blot analyses was carried out and the result revealed the different levels of SVCT2 expression in these CRC cells. HCT8 and HCT116 cells had low expression, while SW620, SW480, and LoVo cells had high expression of SVCT2 (Fig. 1a and Fig. S2). Quantitative analysis also showed distinct expression patterns in these cells (Fig. 1b).

In vitro findings for ^{18}F -DFA cellular uptake showed that the rate of uptake in SW480, SW620, and LoVo cells was significantly higher (approximately 2–4 folds) than that in HCT116 and HCT 8 cells ($t = 8.683$, $P < 0.001$; Fig. 1c). Linear regression analysis showed that the protein expression of SVCT2 was positively associated with tumor cellular uptake of AA in CRC cells ($r = 0.787$, $P < 0.001$; Fig. 1d).

Substrate competitive inhibition studies were carried out in the presence of structural analogs (L-AA and DHA). Unlabeled AA caused a significant reduction of 88% to 90% in the uptake of ^{18}F -DFA in SW480, SW620, and LoVo cells, whereas a reduced inhibition of 20% to 30% in HCT116 and HCT8 cells. Conversely, unlabeled DHA caused a slight reduction (8% to 17%) in the uptake of ^{18}F -DFA; and most of these slight changes were statistically insignificant (Fig. 1c).

In vivo biodistribution studies

The *in vivo* biodistribution of ^{18}F -DFA was evaluated in normal BALB/c nude mice ($n = 5$ per group). Adrenal glands displayed significantly greater uptake of ^{18}F -DFA than other tissues and organs ($14.2 \pm 2.43\%$ ID/g at 60 min). This result is consistent with the previous *in vivo* AA distribution study [16]. The rapid uptake of ^{18}F -DFA was observed in kidneys, with an initially high concentration which was excreted quickly over time. The liver displayed a moderate uptake of ^{18}F -DFA with a slow elution rate. Radioactive substance was also present in the lungs, intestines, heart, and stomach. However, the tracer uptake in these organs was constant up to 120 min. The radioactivity ratio of tissue to blood was > 1 due to effective blood clearance. In the biological distribution data, it was found that the accumulation of ^{18}F -DFA in the brain was low; from $0.51 \pm 0.25\%$ ID/g at 30 min to $0.67 \pm 0.08\%$ ID/g ($P = 0.2029$) at 120 min after injection. The femur uptake rate slightly increased from $1.02 \pm 0.39\%$ ID/g at 30 min to $1.44 \pm 0.16\%$ ID/g ($P = 0.0415$) at 120 min after injection; implying that the compound underwent defluorination *in vivo* (Table 1 and Fig. S3).

Tracer biodistribution experiments were also conducted in tumor-bearing mice. Dissected tumor tissue detection showed that ^{18}F -DFA accumulated in bilateral tumors and the tumor uptake values were higher than those of the surrounding muscle tissues (SW620: 1.39 ± 0.37 vs. 0.44 ± 0.20 , $P = 0.0028$; HCT8: 1.05 ± 0.17 vs. 0.44 ± 0.20 , $P = 0.0033$). A comparison of the tumor-to-muscle ratio (TMR), showed that SW620 tumors with high SVCT2 expression had a

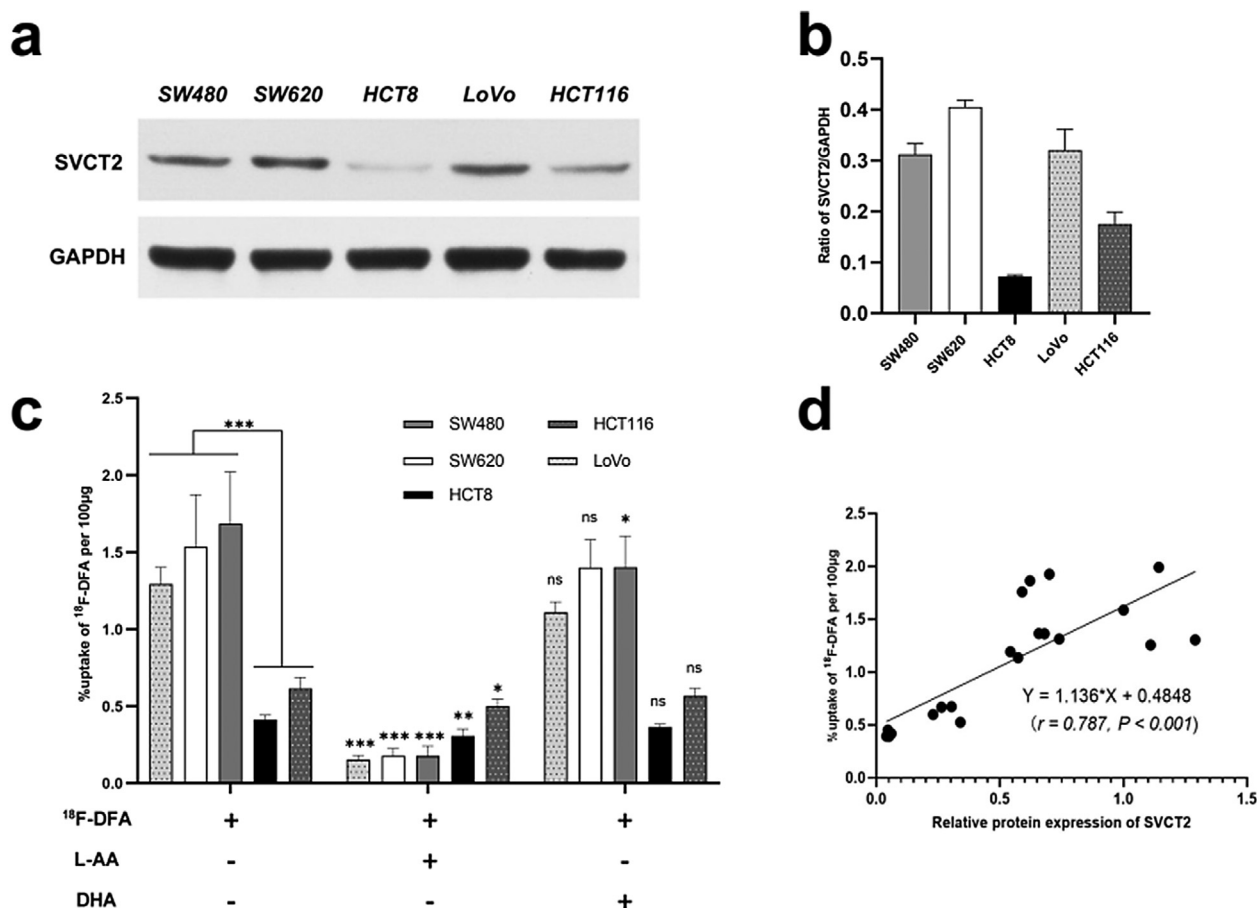


Fig. 1. SVCT-2 expression and uptake of ¹⁸F-DFA with or without structural analogs in different CRC cell lines. (a) SVCT2 expression analyzed using Western blotting. GAPDH was used as a loading control. (b) The ratio of protein expression of SVCT2 to GAPDH quantitatively analyzed. The value of SVCT2 expression is lower in HCT8 and HCT116 cell lines than that in the other three cell lines. (c) Cellular ¹⁸F-DFA uptake in cells treated with or without L-AA or DHA. (d) Linear regression analysis shows significant correlation between protein expression of SVCT2 and uptake of ¹⁸F-DFA in CRC cells ($r = 0.787, P < 0.001$). Data are shown as mean \pm SD. * $P < 0.05$, ** $P < 0.01$ and *** $P < 0.001$, ns = non-significant. ¹⁸F-DFA = 6-Deoxy-6-[¹⁸F] fluoro-L-ascorbic Acid; L-AA = L-ascorbic acid; DHA = dehydroascorbic acid.

higher ratio than in HCT8 tumors which had low SVCT2 expression at 60 min (3.40 ± 0.96 vs. 2.58 ± 0.73 respectively, $P = 0.0345$) (Table 2).

PET imaging of 6-Deoxy-6-[¹⁸F] fluoro-L-ascorbic acid

Dynamic micro-PET scanning was carried out in the tumor-bearing mice to further determine the distribution pattern of ¹⁸F-DFA. For visual observation, animal PET images with a total of 120 min coronal sections were selected. Clear tumor uptake was observed in the animal model (Fig. 2a). The time-activity curve of ¹⁸F-DFA can be drawn by calibrating the ROI in the dynamic images. The tumor-to-brain (TBR) and TMR relative uptake ratios were then calculated at different intervals (Fig. 2b). In the initial 20 min, rapid tumor uptake was visualized and the maximum TBR uptake was reached after the ¹⁸F-DFA injection. The highest SW620 TBR was 17.81 and the highest HCT8 TBR was 12.38. The tumor maintained the tracer with a slow washout rate during the subsequent scan (Fig. 2c and Fig. S4).

The distribution of ¹⁸F-DFA in various organs was observed when the interaction of overlapping tissues and organs *in vivo* was prevented. After dissection, we performed *ex vivo* animal PET experiments in a tumor-bearing mouse. Clear tumor uptake of ¹⁸F-DFA was visualized in the bilateral tumors and the adrenal glands. High uptake of ¹⁸F-DFA was also evident in the lungs, kidneys, and intestines (Fig. 3). This result demonstrated the ability of tumor tissues and other organs to aggregate AA.

Table 2

In tissue biodistribution of 6-Deoxy-6-[¹⁸F] fluoro-L-ascorbic Acid in BALB/c nude mice bearing tumor xenografts after intravenous injection.

Organ	30min	60min
Brain	0.36 \pm 0.09	0.51 \pm 0.12
Blood	0.42 \pm 0.08	0.49 \pm 0.05
Heart	1.11 \pm 0.22	1.17 \pm 0.21
Lung	4.03 \pm 1.64	5.60 \pm 1.69
Liver	5.30 \pm 1.13	5.07 \pm 0.81
Pancreas	1.65 \pm 0.62	1.65 \pm 0.37
Spleen	2.11 \pm 0.46	2.48 \pm 0.73
Adrenals	8.77 \pm 1.07	11.6 \pm 1.26
Kidneys	7.38 \pm 0.71	5.98 \pm 0.45
Intestine	5.91 \pm 1.01	6.92 \pm 1.44
Stomach	2.28 \pm 0.64	2.54 \pm 0.29
Muscle	0.40 \pm 0.14	0.44 \pm 0.20
Bone	0.81 \pm 0.22	1.03 \pm 0.33
Tumor SW620	1.14 \pm 0.27	1.39 \pm 0.37
Tumor to muscle ratio	3.08	3.40
Tumor to blood ratio	2.70	2.94
Tumor HCT8	0.70 \pm 0.33	1.05 \pm 0.17
Tumor to muscle ratio	1.78	2.58
Tumor to blood ratio	1.61	2.17

Data represented as %ID/g, mean \pm SD (5 mice per time point).

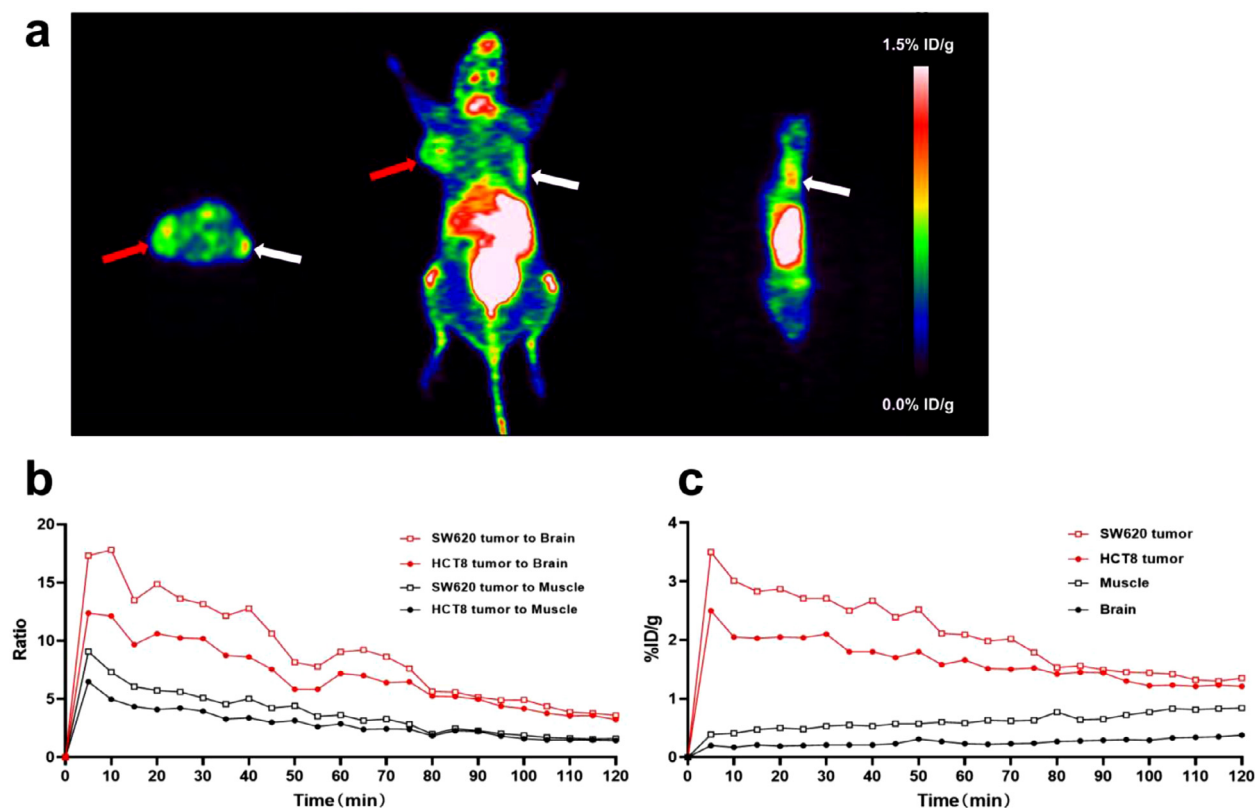


Fig. 2. Static micro-PET images, dynamic time-activity curve, and relative tracer uptake ratio in tumor-bearing mice. (a) Small-animal PET images of ^{18}F -DFA in bilateral tumor-bearing mice at 60 min after intravenous injection. Images are shown in transverse, coronal, and sagittal views. Arrows represent the location of tumors (white arrow shows the SW620 tumor and red arrow shows the HCT8 tumor). (b) Relative uptake ratios of tumor-to-brain (TBR) and tumor-to-muscle (TMR) at different time points (0 to 120 min) after injection with ^{18}F -DFA. (c) Time-activity curves of the brain, muscle, and tumors on tracer uptake in BALB/c nude mice bearing HCT8 and SW620 tumors after injection of ^{18}F -DFA. % ID/g = percent injected dose per gram.

Immunohistochemical analysis

After bilateral tumors resection, a series of pathological procedures were performed. The results of immunohistochemistry showed that SVCT2 was overexpressed in SW620 tumors; and pathological sections showed more intense brown staining of SVCT2 in the cytosol and membrane. In contrast, SVCT2 staining was less in HCT8 tumors (relative positive level ratio: 100.00 ± 113.47 vs. 47.28 ± 40.44 ; $P = 0.0086$, Fig. 4b). Fig. 4a shows representative histopathological images.

Discussion

CRC is one of the most common malignant tumors, with the third highest incidence and the second highest mortality in developed countries [28]. The level of diagnosis and treatment for patients with CRC have undergone significant advances during the past decades. However, the efficacy of chemotherapy is still limited, and drug resistance often occurs in CRC [29]. Therefore, there is an urgent need to provide new therapeutic strategies for patients with advanced CRC to improve their sensitivity to conventional therapeutic agents.

AA was first identified to have anticancer effect in the 1970s [3]. Several studies and clinical trials have shown that high-dose AA alone or in combination with other chemotherapeutic drugs is effective in the treatment of various human cancers [30–32]. AA has almost no toxicity [37] and has attracted great attention to be used as a chemotherapeutic agent [33]. It has been reported that there are approximately a dozen ongoing clinical trials from stage I to III in investigating the high-dose AA as a monotherapy or combination therapy to treat various types of cancers [34]. However, with the development of these clinical trials, there has been controversy. The main controversial point is the lack

of appropriate screening methods to select suitable cancer patients for AA treatment. Among the currently molecular imaging techniques available, PET has been shown to be ideal. For these reasons, we synthesized and labeled the AA analogue, namely ^{18}F -DFA; and focus on the biologic evaluation of ^{18}F -DFA *in vitro* and *in vivo*.

In our study, we observed that tumor cells with high SVCT2 expression had 2–4-fold higher cellular uptake of ^{18}F -DFA than cells with low SVCT2 expression. Although the expression of SVCT2 protein in SW620 is the highest among the five cell lines (Fig. 1b), its uptake rate is not the highest. The possible reason is that the entry of AA into cells mediated by SVCT2 is the main pathway, but it's not the only way [11]. Considering the special redox activity of AA and the subtle effects of different physiological states of cells on AA uptake, the uptake of ^{18}F -DFA might be more complex *in vivo* than that *in vitro*. The inhibition ratio of cells with high SVCT2 expression was almost 90% for 1 mM AA, but not DHA. That's might because ^{18}F -DFA cannot enter the cell through the GLUT pathway since the ^{18}F label in the 6 position prevents formation of the bicyclic species of DHA [19]. Consistent with these results, the study of Varun et al. [35] showed that radiolabeled AA uptake in breast cancer cells was significantly inhibited in the presence of unlabeled AA, whereas no substantial alteration in the uptake was observed with unlabeled DHA.

Animal PET studies using ^{18}F -DFA exhibited the higher uptake and retention in the high SVCT2 expression tumor models in mice. This is also confirmed in our cell uptake experiments and biodistribution experiments. The biodistribution studies in mice showed high levels of radioactivity uptake in adrenal glands, kidneys, liver, and intestines, that are organs known to have a high affinity of AA [36]. *Ex vivo* animal PET study showed that the adrenal glands have an outstanding ability to aggregate AA. Although this phenomenon has been reported

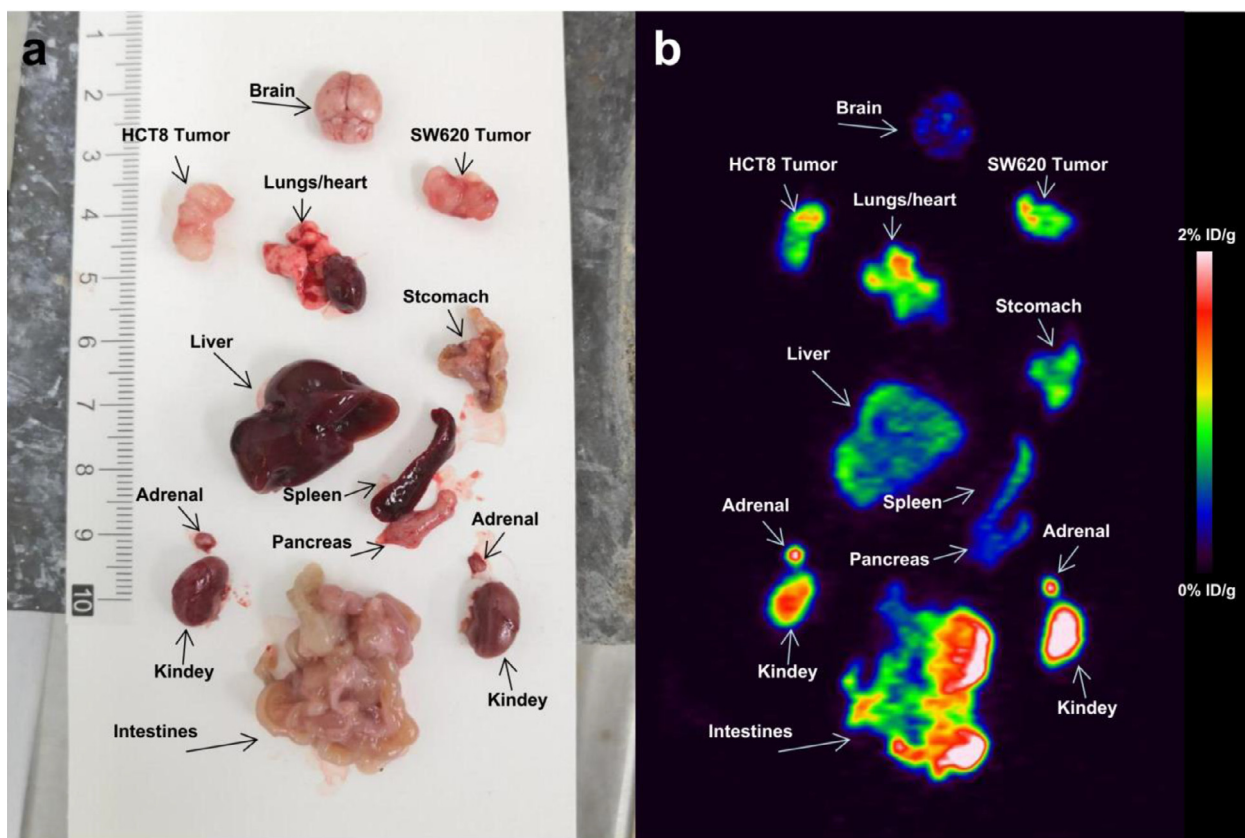


Fig. 3. Ex vivo animal ^{18}F -DFA PET images of a nude mouse bearing SW620 and HCT8 tumor xenografts. Tomographic images obtained by PET (a) were compared to a planar photograph of organs (b).

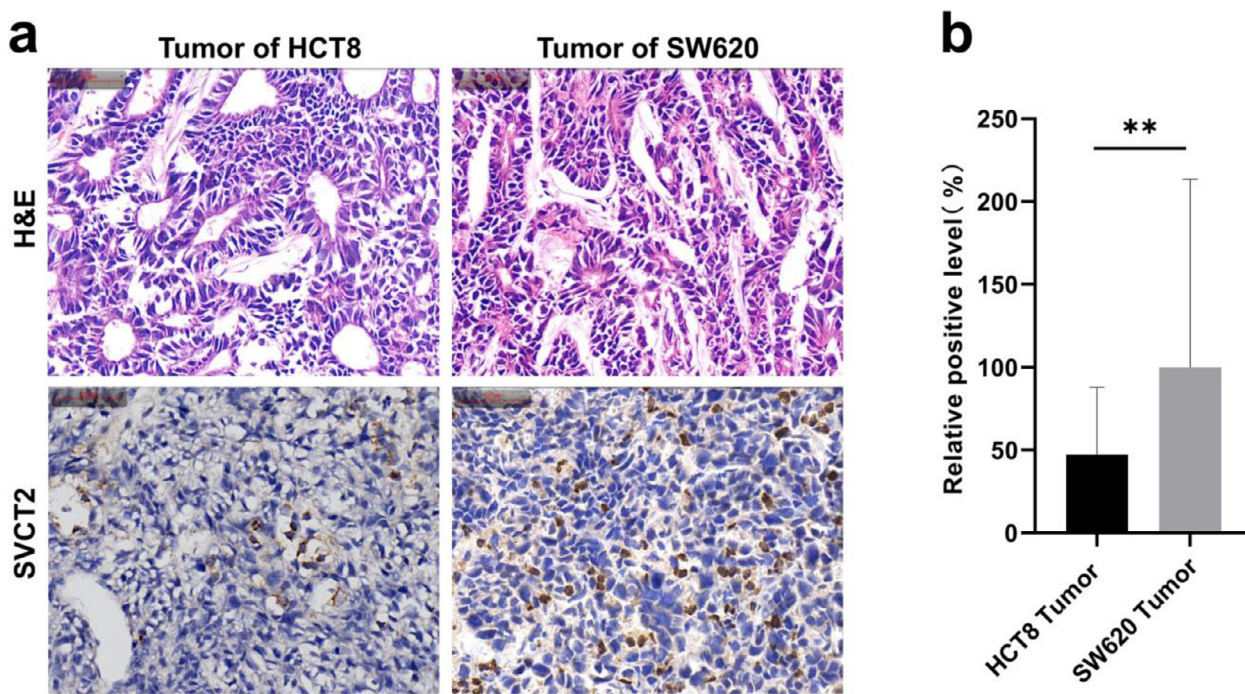
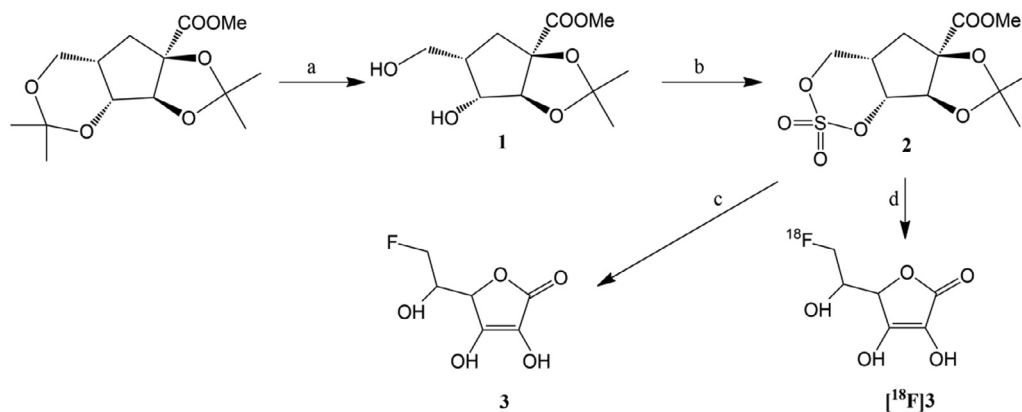


Fig. 4. Representative images of SVCT2 immunohistochemistry and their corresponding H&E staining (a, Right) and statistical graph (b, Left). Immunohistochemistry shows that the expression of SVCT2 (transporter of AA into cells) in SW620 tumor cells is significantly higher than that in HCT8 tumor cells. Scale bar = 50 μm . Data are shown as mean \pm SD ($n = 5$). $**P < 0.01$, $ns =$ not significant.



Scheme 1. Reagent and conditions: (a) (1) $\text{CH}_3\text{I}, \text{K}_2\text{CO}_3$, DMF, rt, overnight; (2) $\text{Cu}(\text{OAc})_2$, H_2O , reflux, 30 min; (b) (1) SOCl_2 , Et_3N , DCM, 0°C , 3 h; (2) RuCl_3 , NaO_4 , CH_3CN , H_2O , rt, overnight; (c) (1) TBAF, THF, 50°C , overnight; (2) 35% HCl, THF, reflux, 2 h; (d) (1) $\text{K}_{222}/\text{K}_2\text{CO}_3/^{18}\text{F}^-$, 10 min; (2) 35% HCl, THF, 10 min.

before [37], to our knowledge, this appears to be the first time that ^{18}F -DFA PET imaging has been used to verify it. The mechanism of high AA uptake in the adrenal glands is still poorly understood. Some studies [38] suggested that the stress response of the adrenal gland to adrenocorticotrophic hormone (ACTH) has been shown to contribute to an increase in the release of AA.

To date, many preclinical studies on the application of AA in the treatment of CRC have achieved gratifying results, but there is no convincing clinical trial result. Some scientists [39] have stated that the re-emerging ascorbate treatment phoenix should be protected instead of being shot down. They strongly encouraged the field to study the potential use of AA, but also sent a cautionary note that new experiments should be properly conducted. The findings of our present study are that SVCT2 overexpression enhanced the uptake of CRC cells to AA, and the tumor-bearing mice were verified by ^{18}F -DFA PET imaging. Based on this, it is expected that the use of a properly prepared ^{18}F -DFA as a radiotracer can provide powerful molecular imaging to support the anticancer research of AA.

Conclusion

Our study suggested that ^{18}F -DFA could be used as a radiotracer to provide powerful imaging information to identify tumors suitable for AA treatment and SVCT2 can be a candidate biomarker in this process. Further clinical trials are warranted to verify the therapeutic efficacy of AA in patients with ^{18}F -DFA high-affinity tumors.

Author contributions

Peng He: Conceptualization, Methodology, Software, Data curation, Writing - Original Draft, Writing-Review & Editing, Visualization, Supervision, Project administration; **Bing Zhang:** Methodology, Software, Writing-Original Draft Preparation and Revised, Funding acquisition; **Yan Zhang:** Radiochemistry, Reviewing and Quality control; **Yuan Zou:** Data analysis, Methodology, Reviewing and Editing; **Yali Long:** Data Curation, Animal experiment; **Jia Qiu:** Data Curation and Animal experiment; **Wanqing Shen:** Data curation, Animal Experiment; **Zhihao Zha:** Radiochemistry; **Xiaoping Lin:** Reviewing, Editing, Technical guidance. **Zhoulei Li:** Reviewing, Editing, Technical guidance and Funding acquisition; **Xiangsong Zhang:** Conceptualization, Reviewing, Editing, Supervision and Funding acquisition.

Declaration of Competing Interest

The authors declare that they have no known competing financial interests or personal relationships that could have appeared to influence the work reported in this paper.

Fundings

This work was supported by the National Science Foundation of China (81901793 and 81602701), the Science and Technology Planning Project of Guangdong Province (2017B020210001), the Training program of the Major Research Plan of Sun Yat-Sen University (17ykjc10), the Science and Technology Program of Guangzhou (201803040020, 201707010110 and 201607010353), Young teacher training program of Sun Yat-sen University (19ykpy55), Project of Nanchong Science and Technology Bureau (19SXHZ0263 and 18SXHZ0385).

Acknowledgments

We are grateful to Xinchong Shi, Renbo Wu, Dake Zhang and Qingqiang Tu for contributions to this project. We thank Qiao Su, Wuguo Li and all members from experimental animal center at the First Affiliated Hospital of Sun Yat-Sen.

References

- [1] M. Levine, New concepts in the biology and biochemistry of ascorbic acid, *New Engl. J. Med.* 314 (14) (1986) 892–902, doi:10.1056/NEJM198604033141407.
- [2] B. Ngo, J.M. Van Riper, L.C. Cantley, J. Yun, Targeting cancer vulnerabilities with high-dose vitamin C, *Nat. Rev. Cancer* 19 (5) (2019) 271–282, doi:10.1038/s41568-019-0135-7.
- [3] J. Yun, E. Mullarky, C. Lu, K.N. Bosch, A. Kavalier, K. Rivera, et al., Vitamin C selectively kills KRAS and BRAF mutant colorectal cancer cells by targeting GAPDH, *Science* 350 (6266) (2015) 1391–1396, doi:10.1126/science.aaa5004.
- [4] A.C. Carr, J. Cook, Intravenous vitamin C for cancer therapy – identifying the current gaps in our knowledge, *Front. Physiol.* 9 (2018) 1182, doi:10.3389/fphys.2018.01182.
- [5] R.W. Welch, Y. Wang, A. Crossman, J.B. Park, K.L. Kirk, M. Levine, Accumulation of Vitamin C (Ascorbate) and its oxidized metabolite dehydroascorbic acid occurs by separate mechanisms, *J. Biol. Chem.* 270 (21) (1995) 12584–12592, doi:10.1074/jbc.270.21.12584.
- [6] C. Wohrlab, E. Phillips, G.U. Dachs, Vitamin C transporters in cancer: current understanding and gaps in knowledge, *Front. Oncol.* 7 (2017) 74, doi:10.3389/fonc.2017.00074.
- [7] A. Godoy, V. Ormazabal, G. Moraga-Cid, F.A. Zúñiga, P. Sotomayor, V. Barra, et al., Mechanistic insights and functional determinants of the transport cycle of the ascorbic acid transporter SVCT2, *J. Biol. Chem.* 282 (1) (2006) 615–624, doi:10.1074/jbc.M608300200.
- [8] C.P. Corpe, H. Tu, P. Eck, J. Wang, R. Faulhaber-Walter, J. Schnermann, et al., Vitamin C transporter SLC23A1 links renal reabsorption, vitamin C tissue accumulation, and perinatal survival in mice, *J. Clin. Invest.* 120 (4) (2010) 1069–1083, doi:10.1172/JCI39191.
- [9] S. Sotiriou, S. Gispert, J. Cheng, Y. Wang, A. Chen, S. Hoogstraten-Miller, et al., Ascorbic-acid transporter SLC23A1 is essential for vitamin C transport into the brain and for perinatal survival, *Nat. Med.* 8 (5) (2002) 514–517, doi:10.1038/0502-514.
- [10] S. Cho, J.S. Chae, H. Shin, Y. Shin, Y. Kim, E. Kil, et al., Enhanced anticancer effect of adding magnesium to vitamin C therapy: inhibition of hormetic response by SVCT-2 activation, *Transl. Oncol.* 13 (2) (2020) 401–409, doi:10.1016/j.tranon.2019.10.017.
- [11] S.W. Hong, S.H. Lee, J.H. Moon, J.J. Hwang, D.E. Kim, E. Ko, et al., SVCT-2 in breast cancer acts as an indicator for L-ascorbate treatment, *Oncogene* 32 (12) (2013) 1508–1517, doi:10.1038/onc.2012.176.

- [12] S. Jung, D. Lee, J. Moon, S. Hong, J. Shin, I.Y. Hwang, et al., L-Ascorbic acid can abrogate SVCT-2-dependent cetuximab resistance mediated by mutant KRAS in human colon cancer cells, *Free Radical Bio. Med.* 95 (2016) 200–208, doi:10.1016/j.freeradbiomed.2016.03.009.
- [13] E. Peña, F.J. Roa, E. Inostroza, K. Sotomayor, M. González, F.A. Gutierrez-Castro, et al., Increased expression of mitochondrial sodium-coupled ascorbic acid transporter-2 (mitSVCT2) as a central feature in breast cancer, *Free Radical Bio. Med.* 135 (2019) 283–292, doi:10.1016/j.freeradbiomed.2019.03.015.
- [14] N. Tahara, A. Tahara, A. Honda, Y. Nitta, N. Kodama, S. Yamagishi, et al., Molecular imaging of vascular inflammation, *Curr. Pharm. Des.* 20 (14) (2014) 2439–2447, doi:10.2174/13816128113199990479.
- [15] F. Yamamoto, S. Sasaki, M. Maeda, Positron labeled antioxidants: synthesis and tissue biodistribution of 6-deoxy-6-[18F]fluoro-L-ascorbic acid, *Int. J. Rad. Appl. Instrum. A* 43 (5) (1992) 633–639, doi:10.1016/0883-2889(92)90032-a.
- [16] T.C. Wilson, M. Xavier, J. Knight, S. Verhoog, J.B. Torres, M. Mosley, et al., PET imaging of PARP expression using 18F-Olaparib, *J. Nucl. Med.* 60 (4) (2019) 504–510, doi:10.2967/jnumed.118.213223.
- [17] J. Kim, F. Yamamoto, S. Gondo, T. Yanase, T. Mukai, M. Maeda, 6-Deoxy-6-[131I]iodo-L-ascorbic acid for the *in vivo* study of ascorbate: autoradiography, biodistribution in normal and hypolipidemic rats, and in tumor-bearing nude mice, *Biol. Pharm. Bull.* 32 (11) (2009) 1906–1911, doi:10.1248/bpb.32.1906.
- [18] J. Kim, T. Kino, H. Kato, F. Yamamoto, K. Sano, T. Mukai, M. Maeda, 5-O-(4-[125I]iodobenzyl)-L-ascorbic acid: electrophilic radioiodination and biodistribution in mice, *Chem. Pharm. Bull. (Tokyo)* 60 (2) (2012) 235–240, doi:10.1248/cpb.60.235.
- [19] D. Hornig, F. Weber, O. Wiss, Uptake and release of [I-14C]ascorbic acid and [I-14C]dehydroascorbic acid by erythrocytes of guinea pigs, *Clin. Chim. Acta* 31 (1) (1971) 25–35, doi:10.1016/0009-8981(71)90358-5.
- [20] V.N. Carroll, C. Truillet, B. Shen, R.R. Flavell, X. Shao, M.J. Evans, et al., [11C]Ascorbic and [11C]dehydroascorbic acid, an endogenous redox pair for sensing reactive oxygen species using positron emission tomography, *Chem. Commun.* 52 (27) (2016) 4888–4890, doi:10.1039/C6CC00895J.
- [21] J. Madaj, Y. Nishikawa, V.P. Reddy, P. Rinaldi, T. Kurata, V.M. Monnier, 6-Deoxy-6-fluoro-L-ascorbic acid: crystal structure and oxidative degradation, *Carbohydr. Res.* 329 (2) (2000) 477–485, doi:10.1016/S0008-6215(00)00183-X.
- [22] S.C. Rumsey, R.W. Welch, H.M. Garraffo, P. Ge, S. Lu, A.T. Crossman, et al., Specificity of ascorbate analogs for ascorbate transport, *J. Biol. Chem.* 274 (33) (1999) 23215–23222, doi:10.1074/jbc.274.33.23215.
- [23] M. Maeda, T. Fukumura, M. Kojima, The dimethylsulfonium moiety as a leaving group in aromatic radiofluorination using tetra-n-butylammonium [18F]fluoride, *Appl. Radiat. Isotopes* 38 (4) (1987) 307–310, doi:10.1016/0883-2889(87)90046-3.
- [24] H.H. Coenen, M. Schüller, G. Stöcklin, B. Klatte, A. Knöchel, Preparation of N.C.A. [17-18F]-fluoroheptadecanoic acid in high yields via aminopolyether supported, nucleophilic fluorination, *J. Labelled Compd. Rad.* 23 (2) (1986) 455–466, doi:10.1002/jlcr.2580230502.
- [25] J. Kiss, K.P. Berg, A. Dirscherl, W.E. Oberhänsli, W. Arnold, Synthese und Eigenschaften von 6-Desoxy-6-halogen-Derivaten derL-Ascorbinsäure, *Helv. Chim. Acta* 63 (6) (1980) 1728–1739, doi:10.1002/hlca.19800630642.
- [26] S. Cho, J.S. Chae, H. Shin, Y. Shin, H. Song, Y. Kim, et al., Hormetic dose response to L-ascorbic acid as an anti-cancer drug in colorectal cancer cell lines according to SVCT-2 expression, *Sci. Rep.* 8 (1) (2018) 11372, doi:10.1038/s41598-018-29386-7.
- [27] S. Liu, H. Ma, Z. Zhang, L. Lin, G. Yuan, X. Tang, et al., Synthesis of enantiopure 18F-trifluoromethyl cysteine as a structure-mimetic amino acid tracer for glioma imaging, *Theranostics* 9 (4) (2019) 1144–1153, doi:10.7150/thno.29405.
- [28] R.L. Siegel, K.D. Miller, A. Goding Sauer, S.A. Fedewa, L.F. Butterly, J.C. Anderson, et al., Colorectal cancer statistics, 2020, *CA Cancer J. Clin.* 70 (3) (2020) 145–164, doi:10.3322/caac.21601.
- [29] C. Cremolini, F. Loupakis, C. Antoniotti, C. Lupi, E. Sensi, S. Lonardi, et al., FOLFOXIRI plus bevacizumab versus FOLFIRI plus bevacizumab as first-line treatment of patients with metastatic colorectal cancer: updated overall survival and molecular subgroup analyses of the open-label, phase 3 TRIBE study, *The Lancet Oncol.* 16 (13) (2015) 1306–1315, doi:10.1016/S1470-2045(15)00122-9.
- [30] B.G. Allen, K.L. Bodeker, M.C. Smith, V. Monga, S. Sandhu, R. Hohl, et al., First-in-human phase I clinical trial of pharmacologic ascorbate combined with radiation and temozolomide for newly diagnosed glioblastoma, *Clin. Cancer Res.* 25 (22) (2019) 6590–6597, doi:10.1158/1078-0432.CCR-19-0594.
- [31] J.D. Schoenfeld, Z.A. Sibenaller, K.A. Mapuskar, B.A. Wagner, K.L. Cramer-Morales, M. Furqan, et al., O₂ ·- and H₂O₂ ·-Mediated Disruption of Fe metabolism causes the differential susceptibility of NSCLC and GBM cancer cells to pharmacological ascorbate, *Cancer Cell* 31 (4) (2017) 487–500 e8, doi:10.1016/j.ccell.2017.02.018.
- [32] S.J. Padayatty, H. Sun, Y. Wang, H.D. Riordan, S.M. Hewitt, A. Katz, R.A. Wesley, M. Levine, Vitamin C pharmacokinetics: implications for oral and intravenous use, *Ann. Intern. Med.* 140 (7) (2004) 533–537, doi:10.7326/0003-4819-140-7-200404060-00010.
- [33] H. Fritz, G. Flower, L. Weeks, K. Cooley, M. Callachan, J. McGowan, et al., Intravenous vitamin C cancer, *Integr. Cancer Ther.* 13 (4) (2014) 280–300, doi:10.1177/1534735414534463.
- [34] G. Nauman, J. Gray, R. Parkinson, M. Levine, C. Paller, Systematic review of intravenous ascorbate in cancer clinical trials, *Antioxidants* 7 (7) (2018) 89, doi:10.3390/antiox7070089.
- [35] V. Khurana, D. Kwatra, D. Pal, A.K. Mitra, Molecular expression and functional activity of vitamin C specific transport system (SVCT2) in human breast cancer cells, *Int. J. Pharmaceut.* 474 (1–2) (2014) 14–24, doi:10.1016/j.ijpharm.2014.07.056.
- [36] D. Hornig, Distribution of ascorbic acid, metabolites and analogues in man and animals, *Ann. N.Y. Acad. Sci.* 258 (1975) 103–118, doi:10.1111/j.1749-6632.1975.tb29271.x.
- [37] H. Tsukaguchi, T. Tokui, B. Mackenzie, U.V. Berger, X.Z. Chen, Y. Wang, et al., A family of mammalian Na⁺-dependent L-ascorbic acid transporters, *Nature* 399 (6731) (1999) 70–75, doi:10.1038/19986.
- [38] M.H. Hooper, A. Carr, P.E. Marik, The adrenal-vitamin C axis: from fish to guinea pigs and primates, *Crit. Care* 23 (1) (2019) 22–29 29-2, doi:10.1186/s13054-019-2332-x.
- [39] N. Shenoy, E. Creagan, T. Witzig, M. Levine, Ascorbic acid in cancer treatment: let the phoenix fly, *Cancer Cell* 34 (5) (2018) 700–706, doi:10.1016/j.ccell.2018.07.014.